

****FULL TITLE****

*ASP Conference Series, Vol. **VOLUME**, © **YEAR OF PUBLICATION***
****NAMES OF EDITORS****

Survey Spectroscopy in the Submillimeter and Millimeter, from the CSO to CCAT

C.M. Bradford^{1,2}, J.E. Aguirre^{3,4}, J.J. Bock^{1,2}, L. Earle³, J. Glenn³, H. Inami⁵, P.R. Maloney³, H. Matsuhara⁵, B.J. Naylor^{2,1}, H.T. Nguyen¹, J. Zmuidzinas^{2,1}

Abstract. I outline some results from the Z-Spec instrument at the CSO and present a concept for CCAT survey spectrometer.

1 Introduction

It is a pleasure to present some recent work at this symposium in honor of Tom. One of the hallmarks of Tom's directorship of the CSO has been his support for developing and fielding new instruments built in university-style research efforts. There is no guarantee of a successful outcome in these endeavors, and instrument commissioning takes time from what could otherwise be productive observations with existing instruments, but it is through new measurements that the field is advanced. The (sub)millimeter is particularly exciting since it has been and remains a technical frontier. Tom was one of the early pioneers in millimeter-wave spectroscopy in the early 1970s, and we are still far from the limit of coupling all available telescope throughput ($A\Omega$) with background-limited sensitivity over the full atmospheric bands with useful spectral resolution. Until that limit is reached, substantial scientific gains can be made with instrumentation advances offering a combination of improved sensitivity, wider fields and/or wider bandwidths. In particular, wideband spectroscopy in the (sub) millimeter has been almost completely unexplored. There are several astrophysical diagnostics of the gas-phase ISM available in these bands (see Figure 1), but their observation has been limited to one transition at a time.

2 Z-Spec

Z-Spec offers an advance in bandwidth by using a technique not generally employed in the millimeter: a diffraction grating. The instrument was developed

¹ Jet Propulsion Laboratory, Pasadena, CA, 91109

² California Institute of Technology, Pasadena, CA, 91125

³ University of Colorado, Boulder, CO, 80303

⁴ University of Pennsylvania, Philadelphia, PA, 19104

⁵ Institute for Space and Astronautical Science, Japan Aerospace and Exploration Agency, Sagami, Japan

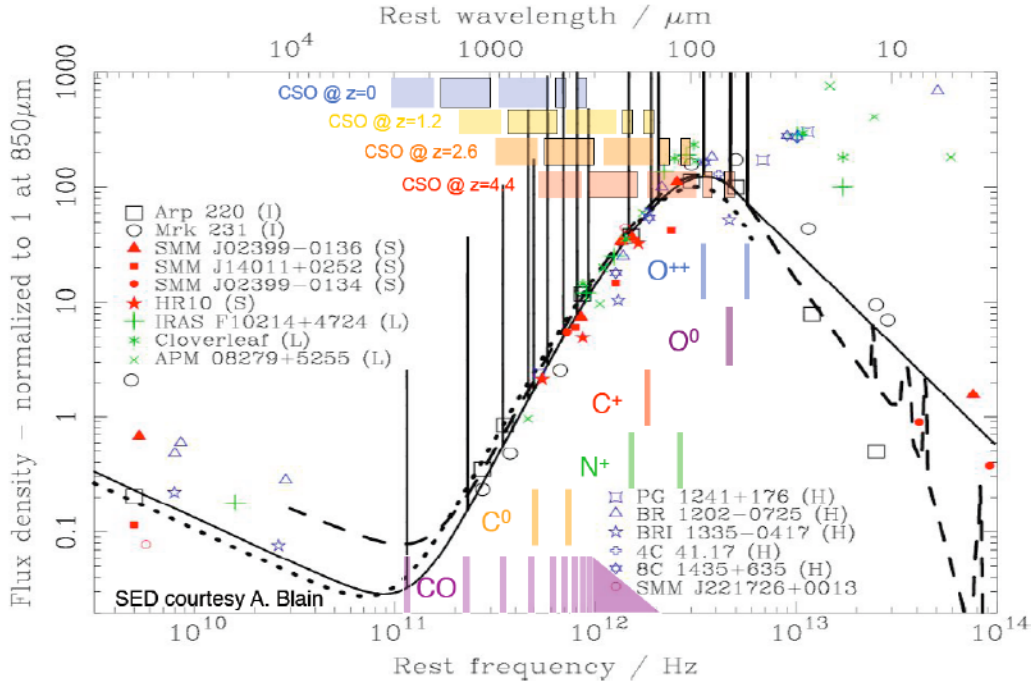


Figure 1. Model spectral energy distribution (SED) from Andrew Blain, with important far-IR / submillimeter / millimeter diagnostics labeled. Redshift ranges corresponding to the atmospheric windows on Mauna Kea are indicated above.

in a collaboration between our group at Caltech / JPL (Jamie Bock, Matt Bradford, Bret Naylor, Hien Nguyen, Jonas Zmuidzinas), Jason Glenn’s group at University of Colorado (with Lieko Earle, James Aguirre (now an Assistant Professor at U. Penn), and Phil Maloney), and Hideo Matsuhara and Hanae Inami at IASA / JAXA in Japan. Z-Spec is a single-beam spectrometer which disperses the 190–308 GHz band across an linear array of 160 bolometers. Traditional grating spectrometers are too large when scaled to the millimeter, so a new approach was required for Z-Spec. It uses a curved grating in a parallel plate waveguide which is fed by a single-mode corrugated feedhorn (Figure 2). Details of the grating design and testing can be found in Naylor et al. (2003); Bradford et al. (2004); Earle et al. (2006); Inami et al. (2008). The resolution of the instrument is modest: limited by practical constraints of the size of a cryostat, as well as detector formats available at the time of its design. The detector spacing increases from ~ 1 part in 400 at the low-frequency end ($\Delta\nu = 500$ MHz), to ~ 1 part in 250 at the high-frequency end of the band ($\Delta\nu = 1200$ MHz), while the spectrometer resolving power runs from ~ 1 part in 300 at low frequencies to ~ 1 part in 250 at the high frequency end of the band. Thus the system is marginally under-sampled, especially at the high-frequencies. Spectral bandpasses for all channels have been measured with a Fourier-Transform spectrometer (FTS) in the laboratory and small adjustments are made based on observations IRC 10216, a multi-line spectral standard. We measure and end-to-end instrument efficiency from outside the cryostat through to absorption in

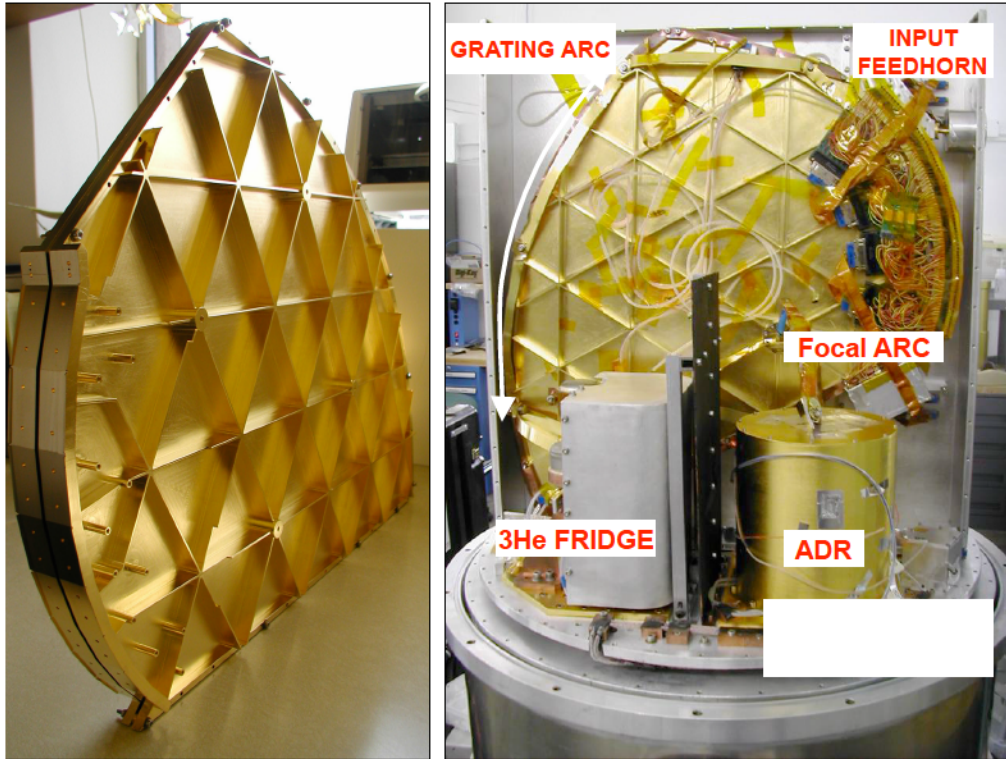


Figure 2. Z-Spec waveguide grating shown edge on (left) and assembled in the cryostat with detectors and the feedhorn / input waveguide (right)

the detectors of 20–30% (in the single-polarization) with absolute DC bolometer measurements (load-curves).

The entire structure is cooled with an adiabatic demagnetization refrigerator and operates at temperatures between 60 and 85 mK to facilitate photon-background-limited detection. A thermal guard at $T \sim 0.5$ K is required, and this cooling is provided by a custom $^3\text{He} / ^4\text{He}$ refrigerator provided by Lionel Duband at CEA-SBT, Grenoble, France. The bolometers were developed at the JPL Microdevices Laboratory; they are individually-mounted silicon-nitride micro-mesh absorbers with quarter-wave backshorts, read-out with neutron-transmutation-doped Germanium thermistors. Detector backgrounds for dispersive spectroscopy in the millimeter are smaller than previous applications. With an operational optical loading is $\sim 1 - 3 \times 10^{-13}\text{W}$, and phonon NEPs of $4 \times 10^{-18}\text{WHz}^{-1/2}$, Z-Spec’s detectors are the most-sensitive, lowest-background bolometers fielded to date for astrophysics.

The instrument mounts at the right-hand Nasmyth platform, fed through the elevation bearing with a relay that de-magnifies the $f/12$ telescope focus to $f/3$ to match to Z-Spec’s input feed (Figure 3). The instrument coupling to the CSO telescope is well-approximated with a Gaussian-beam approach, and we measure beam sizes and instrument efficiencies (via DC load curves on Jupiter) that are consistent with this.



Figure 3. Z-Spec at the CSO in the early commissioning phase with (then) graduate students Bret Naylor and Lieko Earle .

Z-Spec observes in a traditional chop-and-nod mode, with the secondary chopping between 1 and 2 Hz, and a nod period of 20 seconds. Because it is not possible to modulate the spectral response of the instrument relative to the bolometer array, and the spectral resolution elements are not oversampled, it is critical to both insure excellent array yield, and carefully calibrate each detector's response. To address this, we have built a library of planetary observations in varying conditions, and we fit the dependence of each bolometer's response on its operating voltage, a proxy for the combination of bath temperature and optical loading. This relationship provides a calibration correction which is used to bridge intervals between astronomical calibration observations. Based on the self-consistency obtained with this scheme on planets and quasar calibrators, we estimate that the channel-to-channel calibration uncertainties are less than 10%, except at the lowest frequencies which are degraded by the wing of the 186 GHz atmospheric water line.

3 Z-Spec Observational Programs

The Z-Spec team is carrying out observational programs in the local universe and at high redshift. In the local Universe, the 195–305 GHz band hosts low-to mid-J ($J = 2 \rightarrow 1$ to $J = 5 \rightarrow 4$) rotational transitions of several molecular

species including CO and its isotopes, and the well-known density tracers HCN, CN, HNC, HCO⁺, and CS. Taken as an ensemble and with their 100 GHz counterparts, the suite of lines measures mass, density, temperature, and UV or X-ray illumination of the molecular gas. These mm-wave tracers are especially useful for the extremely dusty galaxies which have substantial extinction and line opacity corrections even in the mid- to far-IR. The mm-wave lines suffer no dust extinction, and (other than ¹²CO) are typically optically thin, so they are guaranteed to probe the full bulk of a galaxy's molecular gas. We have observed on the order of a dozen galaxies, ranging from the local starbursts to ULIRGS, with integration times up to 12 hours. Several articles are in the final stages of preparation. We will not present the data here, since they are not yet published, but refer to interested reader to articles on individual sources led by Z-Spec graduate students Naylor et al. (M82), Earle et al. (NGC 253), and Kamenetsky et al. (NGC 1068), which will be in press by the time this volume is published. We also have measurements of more luminous systems (Arp 220, NGC 6240, Mrk 273, Mrk 231) which are being prepared for publication.

Z-Spec was conceived and built with high-redshift observations in mind. As with the submillimeter and millimeter-wave continuum measurements, observations of high-*z* molecular lines benefit from a negative K-correction: the spectral lines generally carry more power at higher frequency. In particular for carbon monoxide, the run of the CO line luminosity with *J* typically increases up to the mid-*J* transitions (*J*~5–10) for actively starforming galaxies. The CO rotational spectrum when measured in energy units thus peaks in the (rest-frame) 200–500 micron range for such sources, and is shifted into Z-Spec's band for redshifts of *z*~1–4. While the detectability of the CO lines depends on the excitation, a rule of thumb is that, in good weather conditions, Z-Spec has the sensitivity to measure CO lines from sources $L_{\text{far-IR}} \sim 3 \times 10^{13} L_{\odot}$ in a night's integration. We are observing both sources with known redshifts (typically lensed) and continuum-selected sources with unknown redshifts in order to conduct the first a priori redshift measurement. The very bright and/or lensed objects are rare, and many nights of data are required for study of more typical sources, and the uncertainties generally to integrate down over multiple nights. We present here some details of our first result, a study of the *z*=2.56 Cloverleaf Quasar, which is in press at the ApJ (astro-ph 0908.1818). (Please refer to the ApJ article rather than these proceedings.) Team member James Aguirre is working on redshift extraction algorithms and we anticipate success with a redshift measurement soon.

4 Z-Spec Cloverleaf Observations

Figure ?? shows the Z-Spec spectrum of the Cloverleaf system. The total integration time is 7.9 hours, split equally over 2 nights, one with excellent weather ($\tau_{225} \sim 0.4 - 0.6$) and one with moderate weather ($\tau_{225} \sim 0.15 - 0.2$). To extract line fluxes, we perform a simultaneous fit to a single component power-law continuum and the multiple lines. Each channel's measured spectral response profile is used in the fitting since the spectrometer is not critically sampled. Four CO lines are clearly detected, though the CI *J*=2→1 ($\nu_{\text{obs}} = 227.5$ GHz) and the CO *J*=7→6 ($\nu_{\text{obs}} = 226.7$ GHz) transitions are separated by only

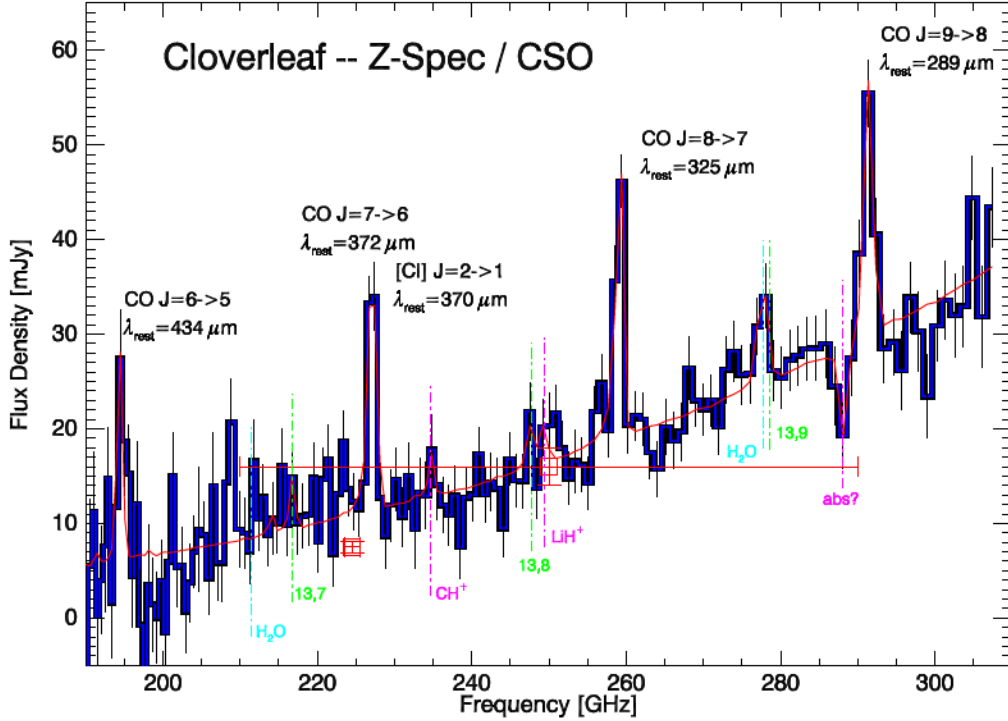


Figure 4. Z-Spec Spectrum toward the $z=2.56$ Cloverleaf Quasar. A fit to the continuum and six spectral lines is overlaid with a light red curve. Red squares with error bars and spectral widths denote continuum measurements from MAMBO and Plateau de Bure. Thin dot-dash lines mark transition frequencies for which upper limits are extracted. The $J = 7 \rightarrow 6$, $J = 8 \rightarrow 7$, and $J = 9 \rightarrow 8$ ^{13}CO frequencies are marked in green with 13,7, 13,8, and 13,9; these upper limits are used in our analysis. Frequencies of the two water transitions with $E_{\text{upper}} < 140$ K in the band are marked in cyan. The LiH and CH^+ frequencies and a tentative absorption feature are marked with magenta; these upper limits can be found in the ApJ article.

1000 km s^{-1} , or about one Z-Spec channel, so blending is a problem. The CO $J=6 \rightarrow 5$, $J=8 \rightarrow 7$, and $J=9 \rightarrow 8$ measurements are the first, and now provide the highest-J CO information in this source, as the CO SED in Figure 5 shows. We compare the CO line ratios (including the ^{13}CO upper limits) to a grid of RADEX radiative transfer models to compute likelihoods for the physical conditions: gas temperature, density, and column density per velocity interval. We find a large mass ($2\text{--}50 \times 10^9 M_{\odot}$) of highly-excited gas with thermal pressure $nT > 10^6 \text{ K cm}^{-3}$.

It is not immediately obvious what is heating the molecular gas around the Cloverleaf. The CO cooling relative to the far-IR dust emission exceeds that in the local starburst galaxies and even ULIRG sources by factors of a few, suggesting that the gas is not originating in photo-dissociation regions around massive stars. The hard X-ray continuum of the active nucleus itself could power the observed CO emission. Hard ($E > 1 \text{ keV}$) X-rays can penetrate a large gas column ($N_{\text{H}} > 10^{22} \text{ cm}^{-2}$) forming an X-ray Dissociation Region (XDR:

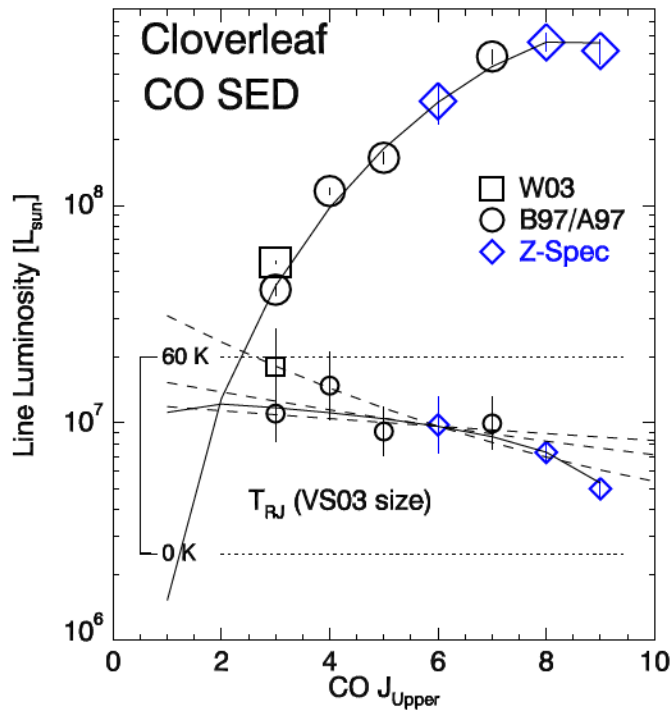


Figure 5. Cloverleaf CO spectrum using all available transitions. The main plot is in bolometric energy units, the inset is in brightness temperature units, referred to the VS03 source size assuming $m = 11$. We have adopted a 20% systematic uncertainty for the measurements other than those from Z-Spec, shown in the temperature plot. A model corresponding to conditions near the peak in the likelihood based on the line ratio analysis ($T = 56$ K, $n_{\text{H}_2} = 2.8 \times 10^4$, cm^{-3} , $N_{\text{CO}}/dv = 1.6 \times 10^6$ $\text{cm}^{-2} \text{km}^{-1} \text{s}$, normalized to match the observed $J = 8 \rightarrow 7$ flux) is overplotted as a solid line in both scales. Dashed lines in the temperature scale show thermalized blackbody emission for temperatures of 25, 50 and 100 K (higher T is shallower slope), arbitrarily normalized to 39 K at $J = 6 \rightarrow 5$. To produce 78% of the total observed intensities (the fraction believed to come from the VS03 disk), the area filling factors relative to the disk would have to be 3.3, 1.1, and 0.46, respectively.

Maloney et al. (1996)). How much X-ray power is available to heat the gas? At the bolometric luminosity estimated for the Cloverleaf AGN ($L_{\text{bol}} \approx 7 \times 10^{13} L_{\odot}$ (Lutz et al. 2007)), the 1 – 20 keV X-rays typically carry $\sim 5\%$ of L_{bol} (Mushotzky et al. 1993) (though with a scatter of a factor of ~ 3 in this relation). This implies that $L_x \approx 3 \times 10^{12} L_{\odot}$; extrapolating to 100 keV with a typical $\nu^{-0.7}$ AGN spectrum would raise this by a factor of 1.6. Thus the hard X-ray luminosity is approaching the 40–120- μm far-infrared luminosity, and

$$\frac{L_{\text{CO}}}{L_x} \approx 10^{-3}.$$

The large column densities derived in the CO-line analysis mean that much of this hard X-ray emission will be absorbed. Unlike in a PDR, the X-rays input a much greater fraction their energy (~ 0.1 – 1) into the gas than the dust, and since the CO lines will be an important coolant, this ratio immediately indicates that the AGN could readily power the CO emission we observe. A detailed XDR model developed by Phil Maloney for this analysis calculates the total CO cooling from X-ray irradiated clouds. When applied to the source size measured with the Plateau de Bure (~ 650 pc) (Venturini & Solomon 2003), we find that the cooling is good match to the observed line fluxes.

X-rays are a bulk heating mechanism and if they are responsible for the heating of the gas, then the properties of the star formation is likely to be very different than in a UV-heated scenario in which shielded cloud cores can cool much more than the irradiated outer regions. Neglecting the effects of magnetic fields and rotation, the mass required for gravitational collapse is given by

$$M_{BE} = \frac{C_{BE} v_T^4}{P^{1/2} G^{3/2}} \propto \frac{T^{3/2}}{n^{1/2}} \propto \frac{T^2}{P^{1/2}}, \quad (1)$$

where T , n , and P are temperature, number density, and thermal pressure, respectively of the environment from which the stars must form, and C_{BE} is a numerical constant. A plausible assertion is that the relevant temperature (perhaps a minimum temperature T_{min}) scales as the typical temperature derived from fits to CO line ratios: at least ~ 50 K per our analysis of the Cloverleaf fluxes, compared with ~ 22 K in the inner Galaxy per the COBE FIRAS measurements (Fixsen et al. 1999). This simple scaling would suggest that M_* in the Cloverleaf starburst is 4–15 times the $0.5 M_\odot$ Galactic value: some 2–5 M_\odot . As Larson (1988) and others have pointed out, such a top-heavy IMF converts a given mass of gas into a greater total stellar (and thus far-IR) luminosity than with the Salpeter IMF. This is the leading scenario proposed to explain the factor of ~ 3 – 5 discrepancy between the observed stellar mass buildup and the star-formation history in the $4 < z < 1$ era (Pérez-González et al. 2008; Davé 2008; Hopkins & Beacom 2006).

5 Spectroscopy with CCAT

Z-Spec operates with photon-noise limited sensitivity at the CSO. Only modest improvements are possible with optimization such as a more efficient instrument, increased resolving power, and/or a second spectrometer to serve as a sky reference. Perhaps a factor of 2 in total might be achieved with a second-generation instrument. The fact is that spectroscopy in the millimeter from a 10-meter telescope can only access the most luminous high-redshift objects. The situation is slightly improved in the short submillimeter, as demonstrated with the ZEUS spectrometer operating at $350 \mu\text{m}$ (Stacey et al. 2007). Here the observed lines are the powerful fine-structure lines (namely [CII], [OI], [OIII]) which are typically an order of magnitude more luminous than the CO lines. Thus, in spite of the increased background, the short submillimeter can be very fruitful band for spectroscopy at $z \sim 1$ – 2 in good Mauna Kea weather. The ZEUS team is reporting several detections of C+ around $z \sim 1.2$ on the CSO in hyperluminous ($L > 10^{13} L_\odot$) sources.

While the so-called ‘negative K-correction’ insures that detectability in the (sub)millimeter is to first order independent of redshift, a 10-meter telescope only probes the very brightest sources and not a typical high-redshift galaxy. What would be a meaningful sample for the high-redshift Universe? Results from Spitzer as well as extrapolations and follow-up of the deep continuum surveys around 1 mm (e.g. Chapman redshifts of SCUBA galaxies) suggest a picture in which dust-enshrouded energy release peaked between redshift 2 and 3, was still very vigorous at $z \sim 1$ (the halfway point in the Universe’s history), and that the typical dusty galaxy at these times had $L \sim 3 \times 10^{11} L_{\odot}$. The density of these sources on the sky is approximately $0.5\text{--}1 \times 10^5$ per square degree, constrained by the total background.

Accessing these populations in the submillimeter requires a substantial advance in the fundamental sensitivities of the observing platform, set by the effective collecting area and the site. ALMA is of course designed for this, and will be capable of measuring spectral lines in typical high- z galaxies. ALMA, however, is not particularly efficient at surveying. The 8–16 GHz of instantaneous bandwidth is much smaller than the ~ 100 GHz atmospheric windows. Moreover, the sky coverage is small: a single primary beam of 6–20 arcseconds couples ~ 1 FIR galaxy except in cases where they are highly clustered. A high-efficiency 25-meter-class single-dish telescope at a high site (CCAT) enables a powerful complement to ALMA: a wideband multi-object survey spectrometer. While a CCAT grating spectrometer is a factor of a few less sensitive than ALMA to a given spectral line in a single source, the bandwidth afforded by the grating can make up the difference for a spectral survey experiment, for either measuring multiple lines or searching for an unknown redshift.

In particular, the $158 \mu\text{m}$ C^+ transition is a promising redshift probe, and, when compared with the total far-IR continuum, can constraint the properties of the starburst (gas density, spatial extent). The telluric windows do not offer complete redshift coverage in C^+ but the 350 and 450 μm windows provide coverage from $z=1\text{--}1.4$ and $1.6\text{--}2.2$, respectively. Evolution models (and the Chapman et al redshift distribution) suggest that these two windows together will likely account for the about one third of all the LIRG-class dusty galaxies. Of course the C^+ coverage increases at higher redshifts as the windows open up. The C^+ fractional luminosity has been a source of some question, as many of the local-universe ULIRGS do show a reduced f_{C^+} relative to the canonical local galaxies, well below 10^{-3} . Of course, as the sources are more luminous, a smaller fractional line luminosity can still represent a large line flux. In the local universe, the measurements suggest a C^+ ‘saturation’ at a line luminosity of $5 \times 10^8 L_{\odot}$ (corresponding to a fractional luminosity of 10^{-3} in a $5 \times 10^{11} L_{\odot}$ source). However, there is increasing evidence that at high redshift, the C^+ fractional luminosity even in powerful sources may be higher, perhaps comparable to that in the local starburst galaxies. Maiolino et al. (2009) is a good recent reference—their Figure 2 suggest a fractional luminosity of 1.3×10^{-3} in ULIRG-class sources at high redshift. The ZEUS team is also reporting ratios higher than the local ULIRGS in their $z \sim 1.2$ measurements.

The real potential for CCAT is in a multi-band, multi-object spectrometer. Figure 6 illustrates the capability of such an instrument on CCAT. While C^+ is typically the easiest transition to detect (in the appropriate redshift windows),

the CO lines are also detectable in the longer-wavelength bands for moderate redshifts. For higher redshifts, the other powerful far-IR lines come in to the short submillimeter bands. This full band could be covered with a suite of 3–4 Z-Spec-like gratings, fed simultaneously through polarizing and dichroic splitters. The resulting package would then be quasi-2-dimensional with a thickness of a few cm, offering the potential to stack multiple spectrometer suites into a single (albeit large) cryostat. The expected density of sources on the sky about one every 10 CCAT 400- μ m beams, is a perfect match to a few-tens-of-object MOS. A warm steerable foreoptics arrangement along the lines of that outlined in Goldsmith & Seiffert (2009) could enable coupling of the spectrometers to the galaxies with good efficiency, so long as they are approximately uniformly distributed. Since even a single object spectrometer rivals ALMA’s survey capability, a 10–100 element multi-object system on CCAT creates a powerful follow-up machine. It would provide wideband spectra of tens of sources per night, revealing redshifts and physical conditions through the rest-frame far-IR and submillimeter spectra, potentially finding interesting objects and/or transitions for detailed study with ALMA.

Acknowledgments. We thank the director and staff of the Caltech Submillimeter Observatory for their ongoing help with Z-Spec. The research described in this (publication or paper) was carried out at the Jet Propulsion Laboratory, California Institute of Technology, under a contract with the National Aeronautics and Space Administration.

References

- Alloin, D., Guilloteau, S., Barvainis, R., Antonucci, R., & Tacconi, L. 1997, *A&A*, 321, 24
- Barvainis, R., Maloney, P., Antonucci, R., & Alloin, D. 1997, *ApJ*, 484, 695
- Bradford, C. M., Ade, P. A. R., Aguirre, J. E., Bock, J. J., Dragovan, M., Duband, L., Earle, L., Glenn, J., Matsuhara, H., Naylor, B. J., Nguyen, H. T., Yun, M., & Zmuidzinas, J. 2004, in *Society of Photo-Optical Instrumentation Engineers (SPIE) Conference Series*, Vol. 5498, *Society of Photo-Optical Instrumentation Engineers (SPIE) Conference Series*, ed. C. M. Bradford, P. A. R. Ade, J. E. Aguirre, J. J. Bock, M. Dragovan, L. Duband, L. Earle, J. Glenn, H. Matsuhara, B. J. Naylor, H. T. Nguyen, M. Yun, & J. Zmuidzinas, 257–+
- Davé, R. 2008, *MNRAS*, 385, 147
- Earle, L., Ade, P., Aguirre, J., Aikin, R., Battle, J., Bock, J., Bradford, C. M., Dragovan, M., Duband, L., Glenn, J., Griffin, G., Hristov, V., Maloney, P., Matsuhara, H., Naylor, B., Nguyen, H., Yun, M., & Zmuidzinas, J. 2006, in *Society of Photo-Optical Instrumentation Engineers (SPIE) Conference Series*, Vol. 6275, *Society of Photo-Optical Instrumentation Engineers (SPIE) Conference Series*
- Fixsen, D. J., Bennett, C. L., & Mather, J. C. 1999, *ApJ*, 526, 207
- Goldsmith, P. F., & Seiffert, M. 2009, *PASP*, 121, 735
- Hopkins, A. M., & Beacom, J. F. 2006, *ApJ*, 651, 142
- Inami, H., Bradford, M., Aguirre, J., Earle, L., Naylor, B., Matsuhara, H., Glenn, J., Nguyen, H., Bock, J. J., Zmuidzinas, J., & Ohyama, Y. 2008, in *Society of Photo-Optical Instrumentation Engineers (SPIE) Conference Series*, Vol. 7020, *Society of Photo-Optical Instrumentation Engineers (SPIE) Conference Series*
- Jappsen, A.-K., Klessen, R. S., Larson, R. B., Li, Y., & Mac Low, M.-M. 2005, *A&A*, 435, 611
- Larson, R. B. 1988, *MNRAS*, 301, 569

- Lutz, D., Sturm, E., Tacconi, L. J., Valiante, E., Schweitzer, M., Netzer, H., Maiolino, R., Andreani, P., Shemmer, O., & Veilleux, S. 2007, *ApJ*, 661, L25
- Maiolino, R., Caselli, P., Nagao, T., Walmsley, M., De Breuck, C., & Meneghetti, M. 2009, *A&A*, 500, L1
- Maloney, P. R., Hollenbach, D. J., & Tielens, A. G. G. M. 1996, *ApJ*, 466, 561
- Mushotzky, R. F., Done, C., & Pounds, K. A. 1993, *ARA&A*, 31, 717
- Naylor, B. J., Ade, P. A. R., Bock, J. J., Bradford, C. M., Dragovan, M., Duband, L., Earle, L., Glenn, J., Matsuhara, H., Nguyen, H., Yun, M., & Zmuidzinas, J. 2003, in *Society of Photo-Optical Instrumentation Engineers (SPIE) Conference Series*, Vol. 4855, *Society of Photo-Optical Instrumentation Engineers (SPIE) Conference Series*, ed. T. G. Phillips & J. Zmuidzinas, 239–248
- Pérez-González, P. G., Rieke, G. H., Villar, V., Barro, G., Blaylock, M., Egami, E., Gallego, J., Gil de Paz, A., Pascual, S., Zamorano, J., & Donley, J. L. 2008, *ApJ*, 675, 234
- Stacey, G. J., Hailey-Dunsheath, S., Nikola, T., Oberst, T. E., Parshley, S. C., Benford, D. J., Staguhn, J. G., Moseley, S. H., & Tucker, C. 2007, in *Astronomical Society of the Pacific Conference Series*, Vol. 375, *From Z-Machines to ALMA: (Sub)Millimeter Spectroscopy of Galaxies*, ed. A. J. Baker, J. Glenn, A. I. Harris, J. G. Mangum, & M. S. Yun, 52–+
- Venturini, S., & Solomon, P. M. 2003, *ApJ*, 590, 740
- Weiß, A., Henkel, C., Downes, D., & Walter, F. 2003, *A&A*, 409, L41

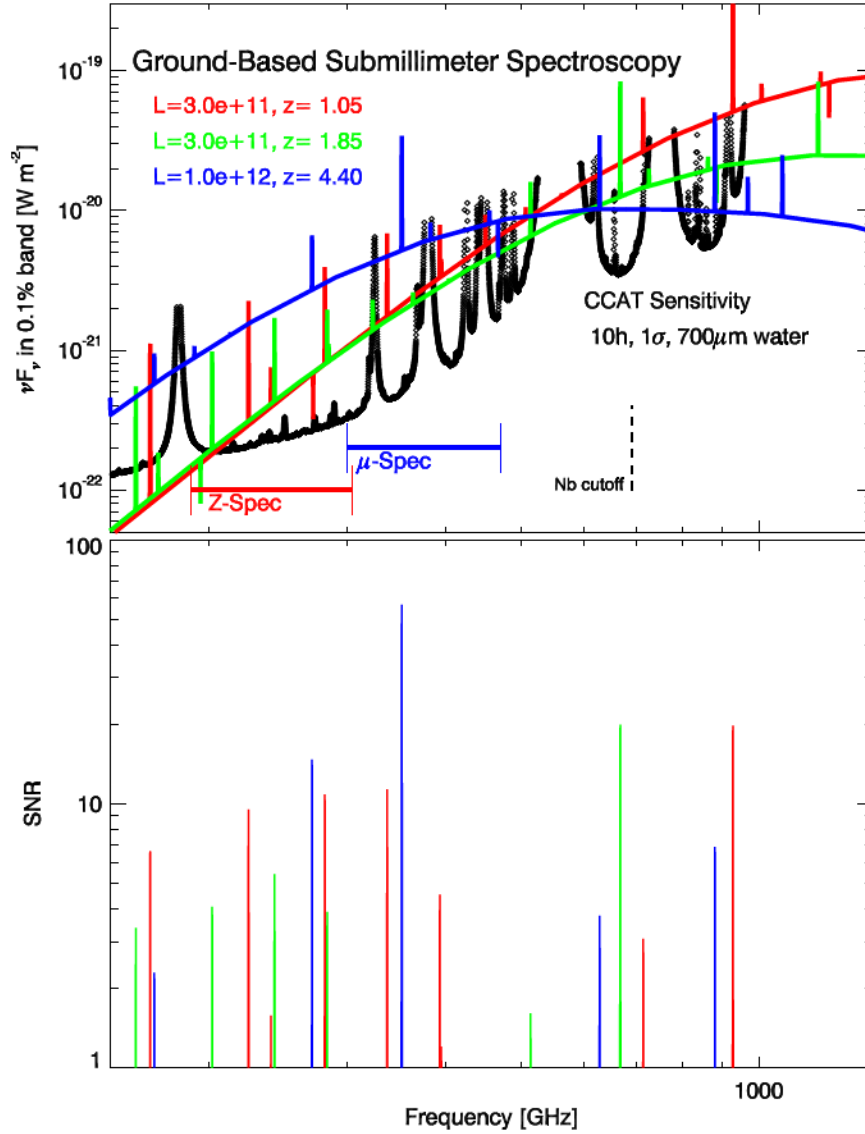


Figure 6. Multiband Spectroscopy with CCAT. Above: heavy black curves show the 1σ sensitivity of a background-limited spectrometer on CCAT assuming a 10-hour integration (chopping included) with flux scale referring to a 1 part in 1000 bandwidth. The forward efficiency is assumed to be 92% and the taper efficiency is assumed to be 88%, and a Ruze efficiency is included assuming surface RMS of $10 \mu m$. The zenith angle is taken to be 0, and $700 \mu m$ of precipitable water vapor is the approximate median. The instrument efficiency is assumed to be 25% in a single polarization, (as per Z-Spec). Colored curves show a model dust + line spectrum scaled to various luminosities ($L_{\text{far-IR}}$), with fine-structure line fractional luminosities ranging up to 2.2×10^{-3} (for [CII]). The Z-Spec spectral coverage, as well as a second fiducial band higher frequency (μ -Spec) are indicated with horizontal bars. A third band could cover both the 650 and 850-GHz windows. Below: signal-to-noise ratio for the spectral lines corresponding to the above model spectra.